Graft Interpenetrating Polymer Networks of Polyurethane and Epoxy Containing Rigid Rods in Side Chain

J. L. Han,[1] S. P. Lin,[2] S. B. Ji,[2] K. H. Hsieh[2]

[1]*Department of Chemical and Materials Engineering, National I-Lan University, I-Lan, Taiwan 260, Republic of China*
[2]*Department of Chemical Engineering, Institute of Polymer Science and Engineering, National Taiwan University, Taipei, Taiwan 106, Republic of China*

Received 29 August 2006; accepted 9 April 2007
DOI 10.1002/app.26874
Published online 17 August 2007 in Wiley InterScience (www.interscience.wiley.com).

ABSTRACT: The rigid rod-like 4,4′-bis(6-hydroxyhexyloxy)biphenyl (BHHBP) units were distributed in either the epoxy or polyurethane to become SR-epoxy and PU (with or without BHHBP) polymer matrices. The interpenetrating polymer networks (IPNs) of PU (with or without BHHBP) and SR-epoxy were synthesized through simultaneous polymerization, and connected each other via the grafting reaction between the —NCO groups of the PU polymer network and the —OH groups on the side chains of SR-epoxy network. The thermal and mechanical characteristics, compatibilities, and morphologies of these PU (with or without BHHBP)/SR-epoxy graft-IPNs were investigated. The polyether-type PU(PPG series)/SR-epoxy graft-IPNs exhibited two-phased morphologies (i.e., phase separation occurred), and higher fracture energies (G_{IC}). Whereas the polyester-type PU(PBA series)/SR-epoxy graft-IPNs were homogeneous (no phase separation), and exhibited higher tensile and Izod impact strengths. © 2007 Wiley Periodicals, Inc. J Appl Polym Sci 106: 3298–3307, 2007

Key words: grafted-interpenetrating polymer networks (graft-IPNs); epoxy; polyurethane (PU); mechanical property; liquid crystal polymer (LCPs); compatibililty

INTRODUCTION

Epoxy resin[1,2] exhibits many advantageous properties, including high processability, low shrinkage, good mechanical, and dielectric properties, and high thermal and chemical resistance. In addition, it displays excellent adhesion to metals, wood, glass, and ceramics. Unfortunately, many products prepared from epoxy resins, which exhibit high glass transition temperatures (T_g) and low toughness, display high brittleness and low impact strength. Because of these drawbacks, much effort has been exerted into the use of low-molecular-weight and soft reactive liquid rubbers[3]—such as carboxyl-terminated butadiene acrylonitrile copolymer (CTBN)—as additives to toughen epoxy resin.[4,5]

Polyurethane (PU), which exhibits urethane(—NH—CO—O—) linkages and was developed in 1937,[6] exhibits many excellent properties that make it suitable for use in many fields. High-purity PU polymers, which possess crystalline or liquid crystalline properties, can be obtained using a variety of synthetic methods and reactants. The development of liquid crystalline polyurethanes (LCPUs) by Iimura et al. in 1981[7] allowed polyurethane materials to be prepared with improved strength. The most important modification method is the use of the TDI/BHHBP system by synthesized BHHBP and 2,4-TDI or 2,6-TDI to the polyether-based LCPUs.[8]

Liquid crystalline polymers (LCP) are used as performance engineering plastics. Because they possess unique mechanical properties, they are receiving considerable attention for use in materials engineering. There is a current trend toward using LCPs as composite reinforcements or matrices. The application of the rigid rod-like structures of LCPs as reinforcements for flexible polymers in molecular composite is another new development.[9–12] The first concept of molecular composites was investigated by the Air Force Materials Laboratory. Since then, many researchers had been exerted into the design and application of related new materials.[13] Nanocomposites possessed a number of advantages over their related macrocomposites, including the use of smaller amounts of the nanoscale dispersion, and excellent high-[14] and low-speed-resistance properties.[15,16] Ionic molecularly modified composites have been prepared by mixing salt-type rigid-rod molecules with a polymer matrix in a cosolvent; the mechanical properties of such composites increased upon increasing

Correspondence to: K. H. Hsieh (khhsieh@ntu.edu.tw).
Contract grant sponsor: National Science Council, Taipei, Taiwan, Republic of China; contract grant number: NSC 89-2216-E-197-003.

Journal of Applied Polymer Science, Vol. 106, 3298–3307 (2007)

TABLE I
Materials

Designation	Description
MDI	4,4′-Diphenylmethane diisocyanate
PPG	Poly(oxypropylene) glycol, MW = 1000
PBA	Poly(butylene adipate) glycol, MW = 1000
Epoxy	Diglycidyl ether of bisphenol A (DGEBA); EEW = 186
TDMP	2,4,6 Tris(dimethylaminomethyl)phenol
TMP	Trimethylolpropane
1,4-BD	1,4-Butanediol
BHHBP	4,4′-Bis(6-hydroxyhexoxyloxy)biphenyl

the degree of rigi-rod reinforcement.[17–19] The addition of rigid rod-like structure of LCPs in polymer matrix exhibited like short fiber reinforced polymer composite.

So the aim of our present research was the preparation of modified epoxy resins containing rigid rod groups and their simultaneous polymerization with polyurethane to form interpenetrating polymer networks (IPNs)[20–23] in an attempt to elevate the properties of the copolymer.[24,25]

EXPERIMENTAL

The materials required for this experiment are listed in Table I. Prior to use, PPG1000, PBA1000, and the epoxy diglycidyl ether of bisphenol A (DGEBA; EEW = 186) were heated and agitated overnight under vacuum to effect their degassing.

Preparation of 4,4′-bis(6-hydroxyhexyloxy) biphenyl

The preparation of BHHBP has been described previously.[2] The reaction was performed according to Scheme 1.

Preparation of an epoxy derivative containing rigid rods in its side chains (SR-epoxy)

DGEBA was placed into a reaction kettle. Dry nitrogen gas was passed through the reaction kettle to remove any air or moisture. A suitable amount of 4,4′-diphenylmethane diisocyanate (MDI) was then poured into the kettle. The reaction temperature was maintained at $\sim$ 80°C while the mixture was agitated vigorously. Sampling was conducted regularly to monitor, through IR spectroscopy, the changes in the appearance of the signal of the isocyanate (—NCO) group (2270 cm^{-1}). When the peak intensity for the isocyanate groups reached half of its original value (with reference to the peak of the 1,4-bisubstituted benzene units at 840 cm^{-1}), the —OH groups on the side chains of the epoxy resin were deemed to have reacted completely with MDI. BHHBP was added into the bottle and the temperature was elevated to 105°C. Again, the signal of the —NCO groups was monitored at 2270 cm^{-1}; when the signal disappeared, the —OH groups of BHHBP were deemed to have reacted completely with the —NCO groups of MDI. The molecular structure of SR-epoxy is illustrated in Scheme 2.

Preparation of polyurethane prepolymers

Polyurethane (PU) prepolymers were prepared through the reactions of MDI with polyols. MDI was first placed into a reaction kettle and heated to its melting state. Suitable amounts of the polyols were then poured into the reaction kettle within the temperature range 65–70°C while stirring under a nitrogen purge. After a few hours, the content of isocyanate groups was measured using the standard *n*-butanediamine titration method;[26] the reaction was terminated when the content reached the theoretical value. The molecular structure of PU prepolymer based on PBA 1000 and PPG 1000 is illustrated in Scheme 3.

Preparation of PU(with BHHBP)/SR-epoxy graft-IPNs

An excess of PU prepolymer was mixed with SR-epoxy with stirring in a four-neck reactor. Sampling was conducted regularly to monitor the changes in the appearance of the signal of the —NCO groups at 2270 cm^{-1}. The —OH groups on the side chains of SR-epoxy reacted with the —NCO groups of the PU prepolymer to form urethane linkages (i.e., graft chains). Thus, the —NCO groups reduced gradually in intensity upon increasing the reaction time. When the peak intensity of the isocyanate group reached a constant value (with reference to the signal of the 1,4-disubstituted benzene units at 840 cm^{-1}), it was deemed that the —OH groups on the side chains of SR-epoxy had reacted completely with the PU prepolymer and that the reaction could be terminated. The degrees of reaction—determined through FTIR spectroscopic analysis—between two different types of PU prepolymer and SR-epoxy resin are listed in Figures 1 and 2.

At this stage, the mixture was placed into a bottle; the crosslinking agent (BHHBP/TMP ratio = 1 : 4) of the PU prepolymer and 1 phr of the curing agent

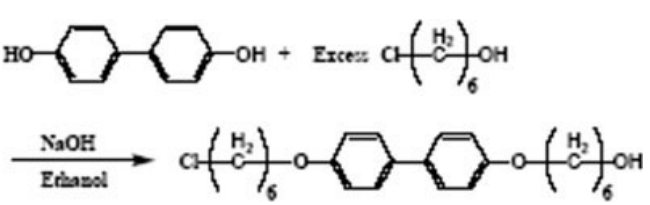

Scheme 1 The synthesis of BHHBP.

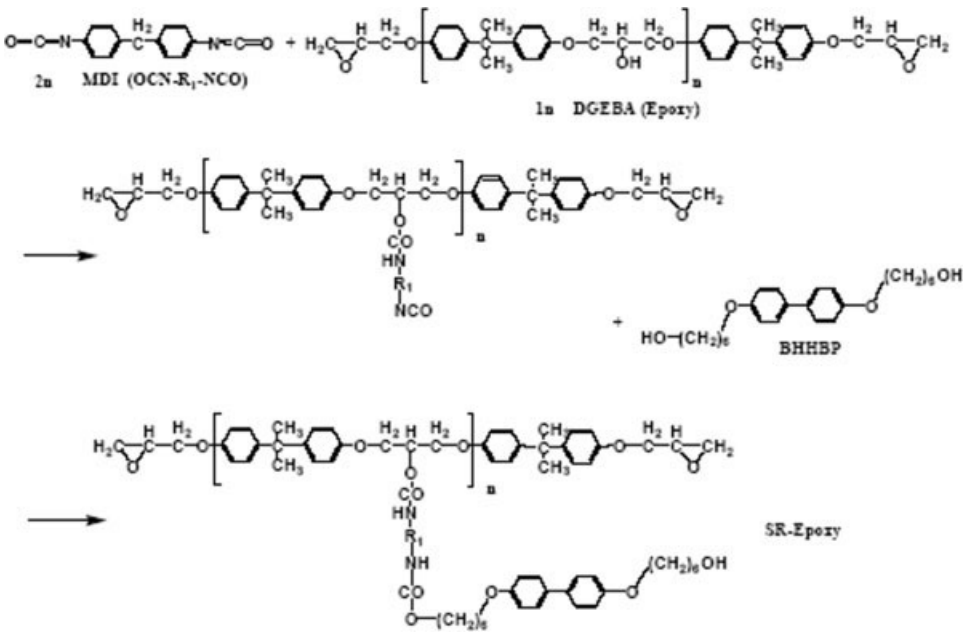

Scheme 2 The molecular structure of SR-epoxy.

(TDMP) of SR-epoxy were added and the mixture was stirred completely. After placing the contents of the bottle under vacuum, the mixture was poured into a hot-press set at 100°C and precured for 1 h; the temperature was then increased to 120°C and curing continued for 8 h. Prior to testing, the samples were stored for three days under an environment having a relative humidity 50%.

The interpenetrating networks of two polymer systems—PU(with BHHBP) and SR-epoxy—could be connected with each other via the grafting reaction between the —NCO groups of the PU polymer network and the —OH groups on the side chains of SR-epoxy network.

Preparation of PU(without BHHBP)/SR-epoxy graft-IPNs

The synthesis procedure including two-stage methods similar to the aforementioned method was used in this system. The mixture of 1,4-butanediol and TMP was applied as the crosslinking agent in the second stage. The molar ratio of 1,4-butanediol and TMP was 1 : 4 in this synthesis step.

Test methods

Infrared spectra were recorded using a BIO-RAD FTS-40 FTIR spectrophotometer operated at a resolution of 4 cm^{-1}. The samples were applied directly onto KBr pellets.

Dynamic mechanical analysis (DMA) was performed using a Du Pont 983 apparatus within an operating temperature range from −120 to +250°C; the heating rate was 5°C/min and the frequency was set at 10 Hz. The samples were $\sim 6 \times 1 \times 0.2$ cm in size.

The stress–strain properties and Izod impact strengths were measured according to the ASTM-D638 and ASTM-D256 methods. The G_{IC} values tests were performed according to the compact tension specimen (CTS) standard method. A number[5–8] of

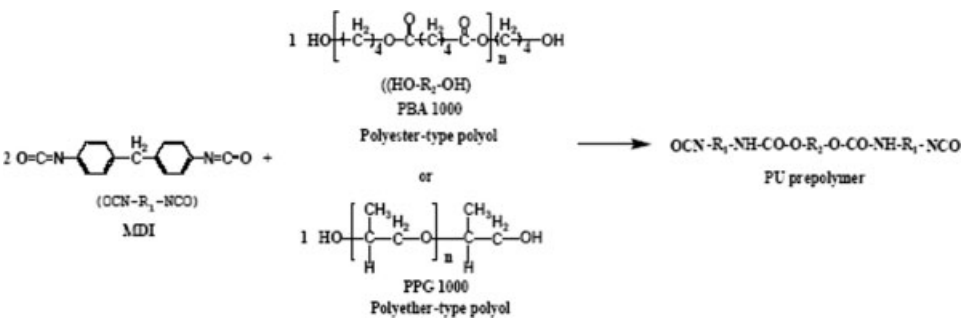

Scheme 3 The molecular structure of PU prepolymer based on PBA 1000 and PPG 1000.

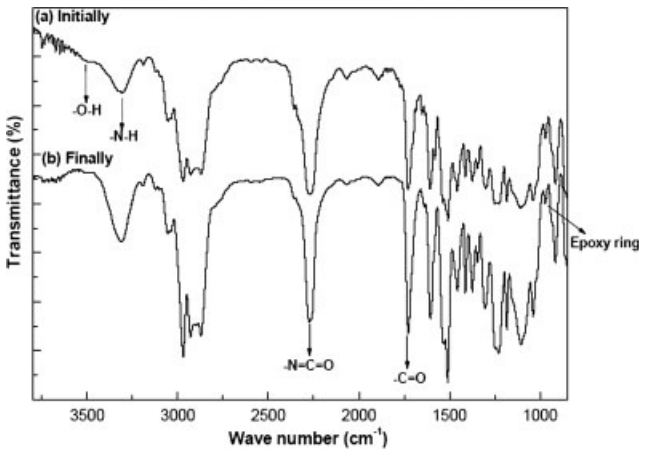

Figure 1 FTIR spectra recorded at the (a) start and (b) end of the reaction between the PU(PPG 1000) prepolymer and the SR-epoxy.

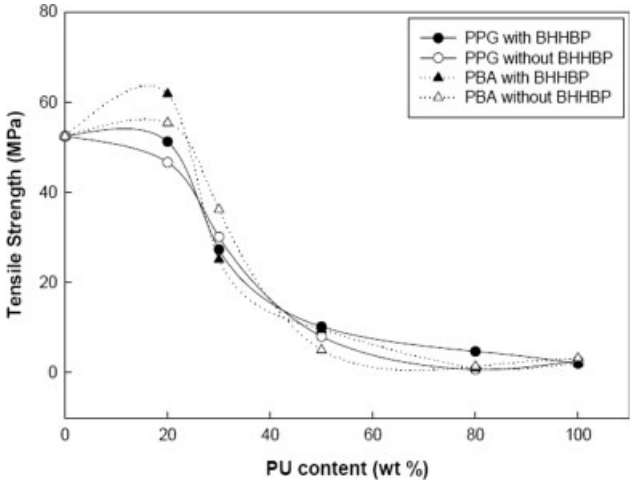

Figure 3 Tensile strengths of PU/SR-epoxy graft-IPNs containing various PU contents.

specimens of each sample were used to obtain average values.

Morphological studies were performed using a scanning electron microscope (SEM). Micrographs of the surface were recorded after fracturing the specimen in liquid nitrogen and then coating it with gold powder.

RESULTS AND DISCUSSION

Stress–strain

Figure 3 and Table II display the relationship between the tensile strength and the content of PU in the PU/SR-epoxy graft-IPNs. For the PU(with BHHBP)/SR-epoxy graft-IPN systems, when the content of PU(with BHHBP) was lower than 20 wt %, the polyester-type PU(PBA with BHHBP)/SR-epoxy graft-IPNs exhibited higher tensile strengths than did the polyether-type PU(PPG with BHHBP)/SR-epoxy graft-IPNs. This phenomenon arose because of the better compatibility between the polyester-type PU(PBA with BHHBP) and SR-epoxy, and because the structures of their graft-IPNs were more complete and had higher crosslinking densities.

When the content of PU(with BHHBP) was higher than 20 wt %; however, the tensile strength of the PU(with BHHBP)/SR-epoxy graft-IPNs decreased upon increasing the content of PU(with BHHBP) because of the increasing content of soft segments of PU. Hence, irrespective of the kind of PU(with BHHBP) adopted, the tensile strengths of the PU(with BHHBP)/SR-epoxy graft-IPNs decreased upon increasing the content of PU(with BHHBP), as shown in Figure 3.

Figure 3 also presents the relationship between the tensile strength and the PU(without BHHBP) content for the PU(without BHHBP)/SR-epoxy graft-IPNs systems. The incompatibility between polyether-type PU(PPG without BHHBP) and SR-epoxy obstructs the formation of IPN structures. The tensile strength of the PU(PPG without BHHBP)/SR-epoxy graft-IPNs decreased upon increasing the content of PU(PPG without BHHBP). For the PU(PBA without BHHBP)/SR-epoxy graft-IPN systems, the tensile strength of PU(PBA without BHHBP)/SR-epoxy graft-IPNs increased initially upon increasing the content of PU(PBA without BHHBP) content up to a maximum value, and then gradually decreased thereafter. The higher compatibility between polyester-type PU(PBA without BHHBP) and SR-epoxy and the existence of the graft chain improved the stability of their IPN structures, but when the PU(PBA without BHHBP) content was too high, the tensile strengths of the PU(PBA without BHHBP)/SR-epoxy graft-IPNs decreased because of the high

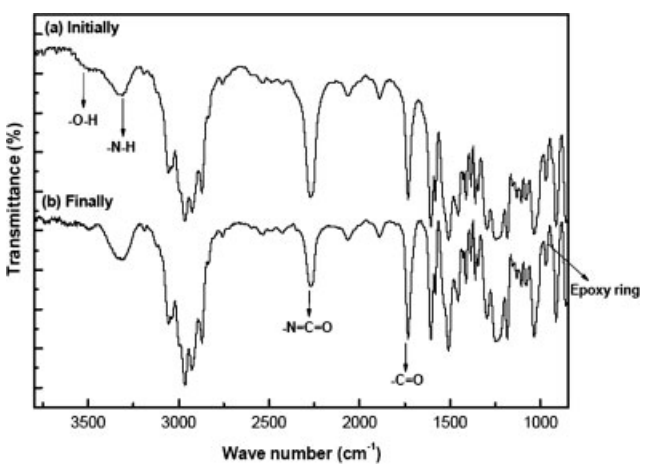

Figure 2 FTIR spectra recorded at the (a) start and (b) end of the reaction between the PU(PBA 1000) prepolymer and the SR-epoxy.

TABLE II
Mechanical Properties of PU/SR-Epoxy Graft-IPNs

PU(with or without BHHBP)/SR-epoxy graft-IPNs			PU content (%) (rigid-rod like BHHBP groups content [wt %])					
			0 (0 wt %)	20 (7.7 wt %)	30 (7.2 wt %)	50 (6.0 wt %)	80 (4.3 wt %)	100 (3.1 wt %)
Tensile strength (MPa)	PU type (PPG 1000)	With BHHBP	52.4	51.2	27.3	10.2	4.7	2.0
		Without BHHBP	52.4	46.6	30.1	8.0	0.7	2.6
	PU type (PBA 1000)	With BHHBP	52.4	61.8	25.1	9.6	1.0	2.1
		Without BHHBP	52.4	55.4	36.2	5.0	1.4	3.2
Izod impact strength (Kgf-m/m)	PU type (PPG 1000)	With BHHBP	4.3	3.4	3.8	2.4	–	–
		Without BHHBP	4.3	4.5	3.5	2.3	–	–
	PU type (PBA 1000)	With BHHBP	4.3	3.6	3.9	2.6	–	–
		Without BHHBP	4.3	5.2	4.8	1.8	–	–
Fracture Energy (KJ m^{-2})	PU type (PPG 1000)	With BHHBP	5.5	7.9	6.4	2.5	–	–
		Without BHHBP	5.5	6.8	6.0	0.7	–	–
	PU type (PBA 1000)	With BHHBP	5.5	6.1	4.7	3.6	–	–
		Without BHHBP	5.5	5.8	5.1	3.8	–	–

abundance of soft segments of PU(PBA without BHHBP).

The dotted lines in Figure 3 indicate that irrespective of the presence of the chain extender mesogenic group BHHBP, the tensile strengths of the PU(PBA)/SR-epoxy graft-IPNs increased upon the addition of PU(PBA) up to a maximum value and then gradually decreased thereafter. The tensile strength of the PU(PBA)/SR-epoxy graft-IPNs was maximized when the PU(PBA) content was 20 wt %. When the content of PU(PBA type) was increased to 20 wt %, the tensile strength of the PU(PBA)/SR-epoxy graft-IPNs system increased because of the compatibility of the polyester-type PU(PBA) and SR-epoxy. When the PU (PBA) content was increased beyond 20 wt %, the tensile strength of the PU(PBA)/SR-epoxy graft-IPNs system decreased because of the increased content of the soft PU(PBA) in the matrix. The solid lines in Figure 3 indicate that the tensile strengths of the PU(PPG)/SR-epoxy graft-IPNs decreased upon increasing the PU(PPG) content as a result of incompatibility between the PU(PPG) and SR-epoxy. Table II lists the tensile strengths of the PU/SR-epoxy graft-IPN systems.

Izod impact strength

Figure 4 and Table II illustrate the relationship between the Izod impact strength and the PU content of the PU/SR-epoxy graft-IPNs. Previously, we proposed that the Izod impact property (i.e., high-shear-rate fracturing) depends on the overall matrix toughness.[27] In the two different polyol-type PU(with BHHBP)/SR-epoxy graft-IPN systems, all of the Izod impact strengths were lower than that of the cured SR-epoxy. In a high-shear-rate fracturing, the rigid-rod structures of the BHHBP groups did not contribute to the Izod impact strength. For the PU(with BHHBP)/SR-epoxy graft-IPN systems, the presence of PU(with BHHBP) aided the formation of graft-IPN structures, but decreased the toughness for the high-shear-rate fracturing (i.e., Izod impact property). The polyester-type PU(PBA with BHHBP)/SR-epoxy graft-IPN systems exhibited higher Izod impact strengths than the polyether-type PU(PPG with BHHBP)/SR-epoxy graft-IPN systems, although they remained lower than that of cured SR-epoxy.

The compatible PU(PBA without BHHBP)/SR-epoxy graft-IPN system is, therefore, the most favorable for improving the Izod impact strength. As indicated in Figure 4, the Izod impact strengths of the PU(PBA without BHHBP)/SR-epoxy graft-IPNs were higher than those of PU(PPG without BHHBP)/SR-epoxy graft-IPNs. In addition, the Izod impact strengths of both graft-IPNs increased initially upon increasing the content of PU(without BHHBP), but thereafter decreased after a maximum value. The Izod impact strengths of the two PU(without BHHBP)/SR-epoxy graft-IPNs at the 20 wt % contents of the polyol-type PU(without BHHBP) poly-

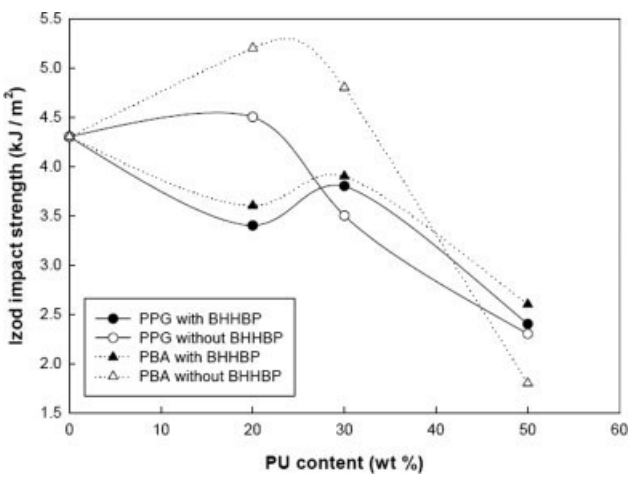

Figure 4 Izod impact strengths of PU/SR-epoxy graft-IPNs containing various PU contents.

mers exceeded that of the cured SR-epoxy; the toughening effect of PU(PBA without BHHBP) was heightened relative to that of PU(PPG without BHHBP) for the PU(without BHHBP)/SR-epoxy graft-IPNs, presumably because the greater compatibility between the polyester-type PU(PBA without BHHBP) and SR-epoxy lead to their forming excellent graft-IPN structures. Even at a high PU(without BHHBP) content (30 wt %), the polyester-type PU(PBA without BHHBP) exhibited excellent Izod impact toughness. In contrast, the PU(PPG without BHHBP)/SR-epoxy graft-IPN systems exhibited phase separation at a high content of polyether-type PU(PPG without BHHBP) (30 wt %), such that no toughening effect occurred in the matrix, leading to a decrease in the Izod impact strength.

To examine the effect of the rigid rod-like BHHBP groups, when the content of PU(PPG without BHHBP) was lower than 20 wt %, the Izod impact strengths of PU(PPG without BHHBP)/SR-epoxy graft-IPNs were higher than that of the cured SR-epoxy, but this situation was not the case for the PU(PPG with BHHBP)/SR-epoxy graft-IPNs. In addition, the Izod impact strengths of the PU(PPG without BHHBP)/SR-epoxy IPNs were also higher than those of the PU(PPG with BHHBP)/SR-epoxy IPNs (see the solid line in Fig. 4). The Izod impact strengths of the PU(PBA without BHHBP)/SR-epoxy graft-IPNs demonstrated that they exhibited greater toughening relative to that of the PU(PBA with BHHBP)/SR-epoxy graft-IPN systems. Therefore, the Izod impact strengths of the PU(PBA without BHHBP)/SR-epoxy graft-IPNs were higher than those of the PU(PBA with BHHBP)/SR-epoxy graft-IPNs (see dotted line in Fig. 4). Table II lists the Izod impact strengths of the PU/SR-epoxy graft-IPNs.

Fracture energy G_{IC}

Figure 5 presents the values of the fracture energy (G_{IC}) of the PU/SR-epoxy graft-IPNs. The maximum value of G_{IC} existed in the PU/SR-epoxy graft-IPNs when the PU content was 20 wt %. Because the toughening behavior of the fracture energy G_{IC} test occurred at a low shear rate, it is important for a precipitate of PU rubber particles to improve the toughness. As mentioned previously,[27] the toughening mechanism for the low-shear-rate fracture test (i.e., measurement of the fracture energy G_{IC}) is different from that of the high-shear-rate fracture test (Izod impact test). A rubber-particle-dispersed matrix usually exhibits a much greater improvement in the fracture energy G_{IC}, because it is more suited to accumulating the energy from reinitiating the cracking of the continuous plastic matrix. As indicated in Figure 5, the values of the fracture energy (G_{IC}) of the polyether-type PU(PPG with BHHBP)/SR-epoxy graft-IPN system were higher than those of the polyester-type PU(PBA with BHHBP)/SR-epoxy graft-IPNs. For the PU(PPG with BHHBP)/SR-epoxy graft-IPNs system (rubber-phase-dispersed matrix), the dual toughening effects that the existence of precipitated PU rubber particles and the addition of the rigid-rod BHHBP groups had on the values of G_{IC} were greater than those in the polyester type PU(PBA with BHHBP)/SR-epoxy graft-IPNs (homogeneous matrix).

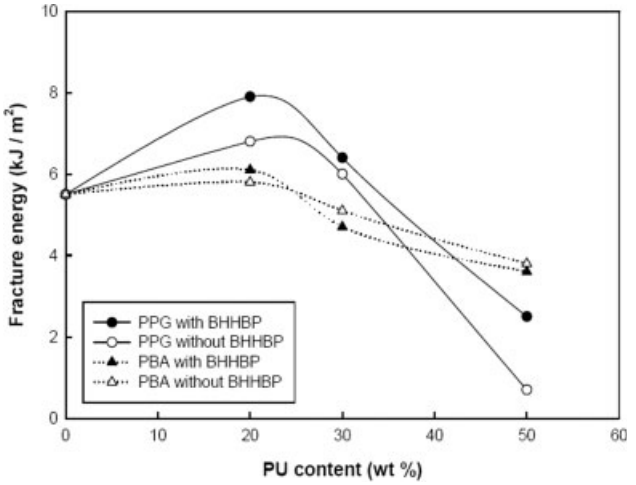

Figure 5 Values of fracture energies (G_{IC}) of PU/SR-epoxy graft-IPNs containing various PU contents.

The fracture energies of the PU(without BHHBP)/SR-epoxy graft-IPN and PU(with BHHBP)/SR-epoxy graft-IPN systems exhibited similar trends. In the polyether-type PU(PPG without BHHBP)/SR-epoxy graft-IPN system, the values of G_{IC} increased because of (a) the PU rubber particle precipitate, (b) the toughening behavior of the fracture energy G_{IC} test performed under a low shear rate, and (c) the fracture front path being resisted by the PU rubber particles and the longer path necessary to complete the fracture behavior. In contrast, the polyester-type PU(PBA without BHHBP)/SR-epoxy graft-IPNs possessed homogeneous phase morphologies and, therefore, their values of G_{IC} were lower than those of the polyether-type PU(PPG without BHHBP)/SR-epoxy graft-IPNs.

The presence of the rigid rod-like BHHBP groups increased the fracture energies of the polyether-type PU(PPG with BHHBP)/SR-epoxy graft-IPN system relative to those of the PU (PPG without BHHBP)/SR-epoxy graft-IPNs, as demonstrated by the solid lines in Figure 5. Irrespective of the presence of the BHHBP groups, at a 20 wt % content of PU(PBA), the values of G_{IC} of the PU(PBA with BHHBP)/SR-epoxy graft-IPNs were higher than those of the PU(PBA without BHHBP)/SR-epoxy graft-IPNs (see the dotted line in Fig. 5). The mesogenic BHHBP

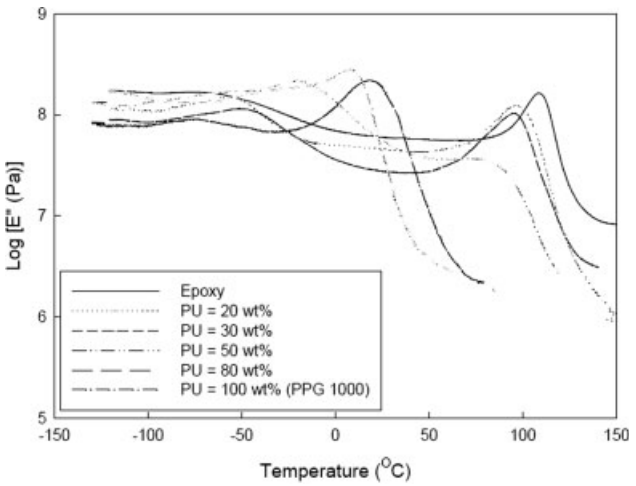

Figure 6 Temperature dependence of log loss moduli (log[E″]) of PU(PPG with BHHBP)/SR-epoxy graft-IPNs containing various contents of PU(PPG 1000): (−) 0 wt %; (. . ...) 20 wt %; (—) 30 wt %; (-..-..-) 50 wt %; (_ _ _) 80 wt %; (-.-.-) 100 wt %.

groups play the role of short fibers that toughen the matrix; their presence improved the low-shear-rate fracture energy, G_{IC}. Table II lists the values of the fracture energies of each of the PU/SR-epoxy graft-IPNs.

Dynamic mechanical analysis

Figures 6 and 7 display the loss moduli (E″) obtained from the DMA of the polyether-type PU(PG with BHHBP)/SR-epoxy graft-IPNs and the polyester-type PU(PBA with BHHBP)/SR-epoxy graft-IPNs, respectively. The epoxy (DGEBA) exhibited one distinct transition which located at 108°C. But two apparent transition regions: a low-temperature transition (T_{gl}) located below −20°C and a high-temperature transition (T_{gh}) located below 100°C were observed in the PU(with BHHBP)/SR-epoxy graft-IPNs systems, representing the molecular motions of PU and SR-epoxy segmental molecules. The IPN structures between the PU and SR-epoxy molecules made the T_{gh} values of two types of PU(with BHHBP)/SR-epoxy graft-IPNs decreased upon increasing the content of PU(with BHHBP). In the polyether-type PU(PPG with BHHBP)/SR-epoxy graft-IPNs system, when the content of PU(PPG with BHHBP) was lower than 50 wt %, the values of T_{gh} decreased upon increasing the content of PU(PPG with BHHBP), whereas the value of T_{gl} increased upon increasing the content of PU(with BHHBP). These phenomena resulted from the effect of phase separation of the PU(PPG with BHHBP)/SR-epoxy graft-IPNs (Fig. 8). In the lower content of PU(with BHHBP), the higher rigid rod-like BHHBP groups aggregated in the soft segmental molecules of PU dispersed phase; as a result, the value of T_{gl} increased upon increasing the PU(with BHHBP) content. This result is consistent with the SEM observation in Figure 8(a–c). In the higher content of PU(with BHHBP), the PU domains became matrix and the lower rigid rod-like BHHBP dispersed uniformly in the PU matrix, as shown in Figure 8(d), so the affecting factor of BHHBP disappeared. For the polyester-type PU(PBA with BHHBP)/SR-epoxy graft-IPNs system, because of the excellent compatibility between the polyester-type PU(PBA) and SR-epoxy resin, the micrographs display homogeneous microstructures (Fig. 9) and the values of T_{gl} were similar; in contrast, the values of T_{gh} decreased upon increasing the content of PU(PBA with BHHBP). Table III illustrates the transition temperatures obtained through DMA of the PU(with BHHBP)/SR-epoxy graft-IPNs.

Compatibility and morphologies

Next, we investigated the morphologies of the polyether-type PU(PPG with BHHBP)/SR-epoxy graft-IPNs and polyester-type PU(PBA with BHHBP)/SR-epoxy graft-IPNs. As indicated in Figure 8, increasing the content of PU(PPG with BHHBP) increased the tendency for phase separation. When the content of PU(PPG with BHHBP) was in the range 20–30 wt %, the PU(PPG with BHHBP) rubber particle size was in the range 0.2–0.5 μm, as illustrated in Figure 8(b,c). These results are consistent with the results of fracture energy G_{IC}, which indicated that the PU(PPG) rubber particle precipitate improved the toughening effect of the low-shear-rate fracture energy G_{IC}. For the polyester-type PU(PBA

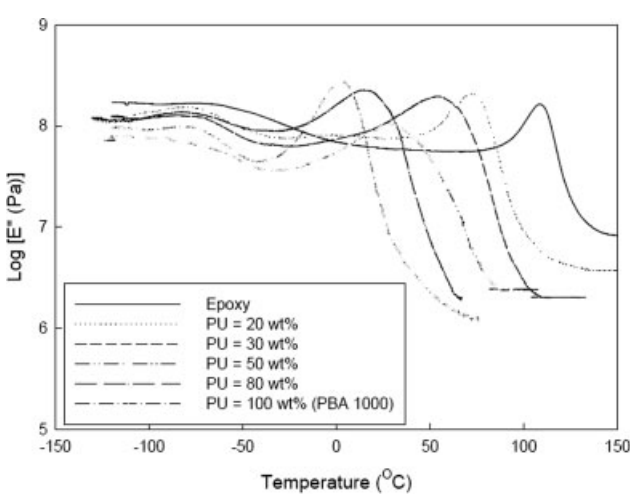

Figure 7 Temperature dependence of log loss moduli (log[E″]) of PU(PBA with BHHBP)/SR-epoxy graft-IPNs containing various contents of PU(PBA 1000): (−) 0 wt % ; (. . ...) 20 wt % ; (—) 30 wt % ; (-..-..-) 50 wt %; (_ _ _) 80 wt %; (-.-.-) 100 wt %.

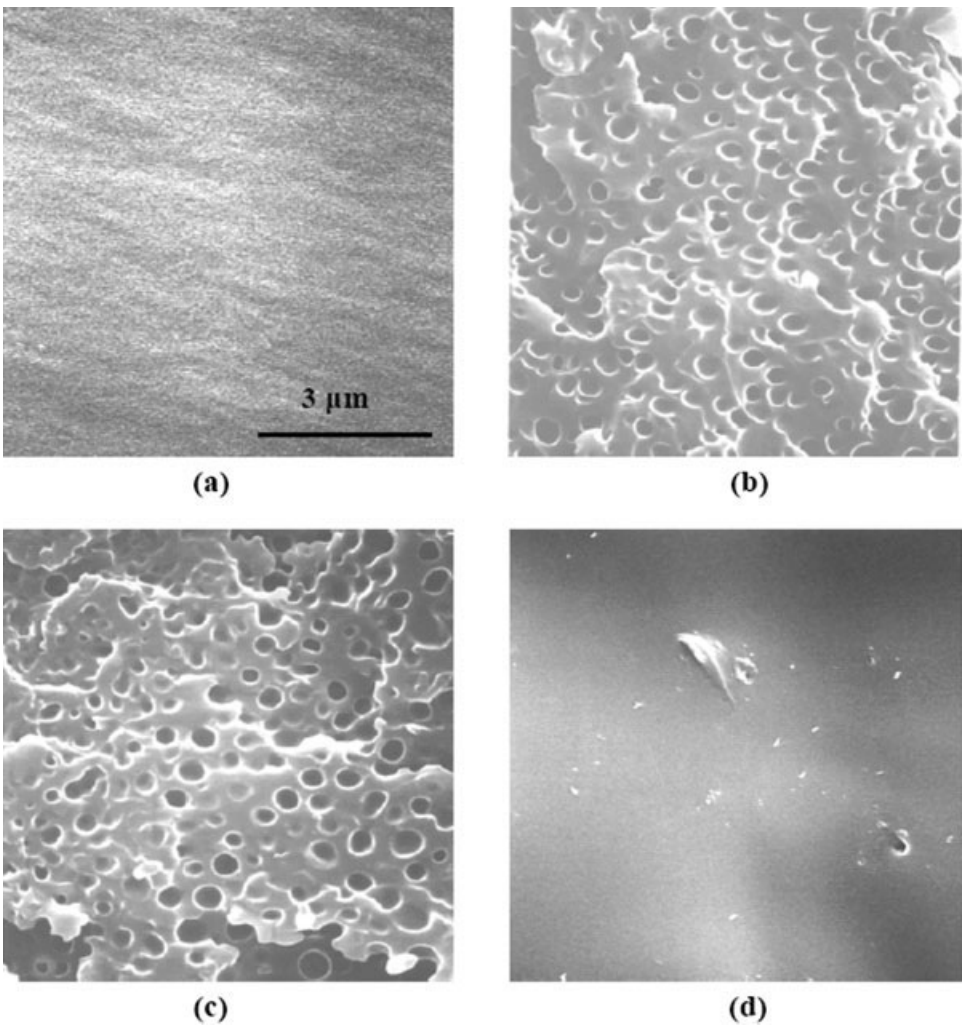

Figure 8 SEM micrographs of PU(PPG with BHHBP)/SR-epoxy graft-IPNs containing various contents of PU(PPG1000): (a) 0 wt %; (b) 20 wt %; (c) 30 wt %; (d) 80 wt %. The scale bar for each image is indicated in Figure 8(a).

with BHHBP)/SR-epoxy graft-IPNs system, the morphology of the microstructure remained homogeneous, irrespective of the content of PU(PBA with BHHBP) (Fig. 9).

CONCLUSIONS

Because of phase separation of the polyether-type PU(PPG with BHHBP)/SR-epoxy graft-IPNs, the higher rigid rod-like BHHBP groups aggregated in the soft segmental molecules of PU dispersed phase; as a result, the value of T_{gl} decreased upon increasing the BHHBP content. For the polyester-type PU(PBA with BHHBP)/SR-epoxy graft-IPNs, the compatibility of the polyester-type PU(PBA) and SR-epoxy resin caused the value of T_{gh} to decrease upon increasing the content of PU(PBA with BHHBP), but the value of T_{gl} did not change significantly. In addition, phase separation in the polyether-type PU(PPG with BHHBP)/SR-epoxy graft-IPNs meant that the values of T_g (derived from DSC analysis) did not change appreciably.

The tensile strength of the polyester-type PU(PBA)/SR-epoxy graft-IPNs increased upon increasing the PU(PBA) content to a maximum value and then decreased gradually thereafter. The maximum tensile strength of the PU(PBA)/SR-epoxy graft-IPNs occurred when the PU(PBA) content was 20 wt %. The polyether-type PU(PPG)/SR-epoxy graft-IPN systems exhibited a tendency of decreasing tensile strength upon increasing the PU(PPG) content, presumably because of incompatibility between the PU(PPG) and epoxy.

The rigid rod-like BHHBP groups did not exert any significant effect on improving the Izod impact strength (high-shear-rate fracture test) of the PU(with BHHBP)/SR-epoxy graft-IPNs; indeed, their presence diminished the Izod impact strength. For the polyether-type PU(PPG without BHHBP)/SR-epoxy

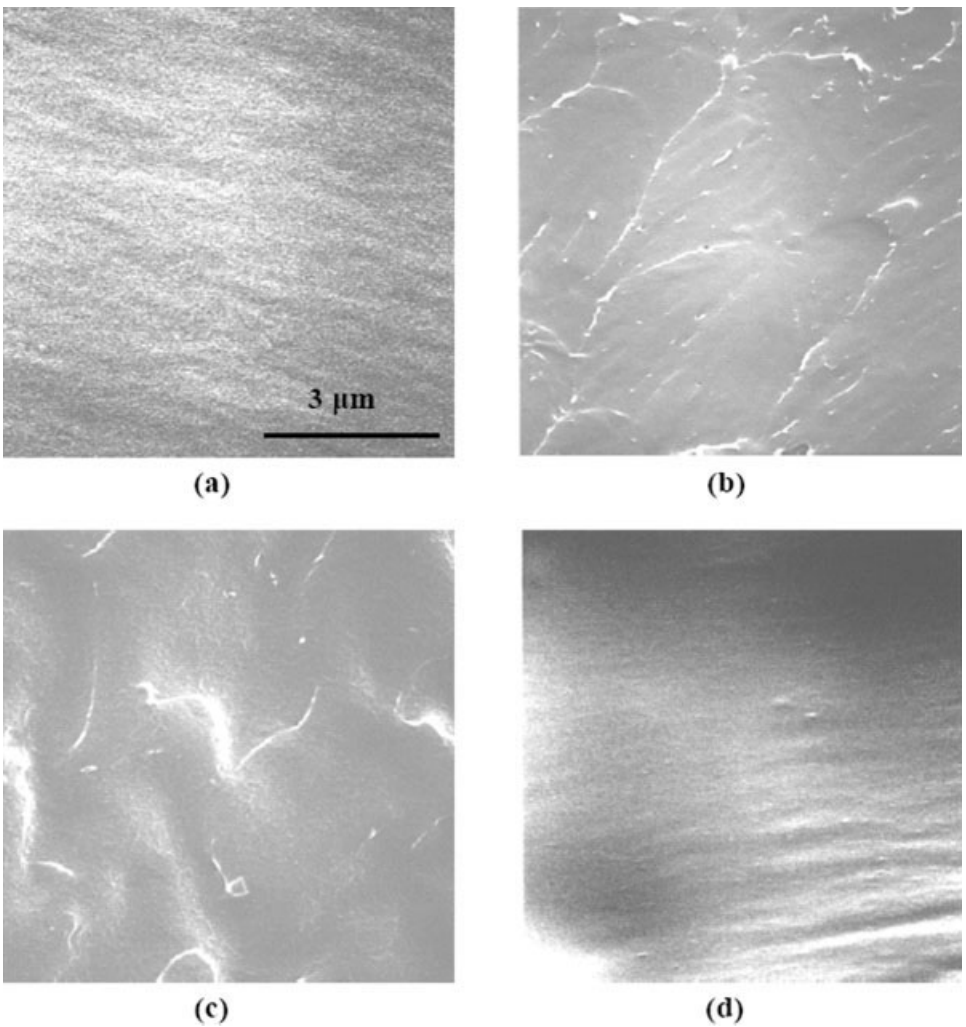

Figure 9 SEM micrographs of PU(PBA with BHHBP)/SR-epoxy graft-IPNs containing various contents of PU(PBA1000): (a) 0 wt %; (b) 20 wt %; (c) 30 wt %; (d) 80 wt %. The scale bar for each image is indicated in Figure 9(a).

graft-IPN systems, the value of the fracture energy G_{IC} test performed under a low shear rate.

The presence of the BHHBP groups improved the fracture energies (low shear rate fracture test, G_{IC}) of the PU/SR-epoxy graft-IPNs because these rigid rod-like units behaved as short fibers that toughened the low-shear-rate fracture behavior of the matrices of the PU/SR-epoxy graft-IPNs.

From a morphological analysis, we found that when the content of PU(PPG with BHHBP) was within the range of 20–30 wt %, the PU(PPG with BHHBP) rubber precipitate had particle sizes within the range of 0.2–0.5 μm. The polyester-type PU(PBA with BHHBP)/SR-epoxy graft-IPNs maintained homogeneous microstructures, irrespective of the content of PU(PBA with BHHBP).

TABLE III
Dynamic Mechanical Analysis of PU (with BHHBP)/SR-Epoxy Graft-IPNs

PU content (%) [rigid-rod like BHHBP content (wt %)]	PU (PPG 1000)		PU (PBA 1000)	
	T_{gh} (°C)	T_{gl} (°C)	T_{gh} (°C)	T_{gl} (°C)
0 (0 wt %)	108.0	−73.1	108.0	−73.1
20 (7.7 wt %)	96.1	−57.6	73.5	−80.2
30 (7.2 wt %)	95.8	−49.5	54.3	−76.5
50 (6.0 wt %)	71.8	−19.7	28.3	–
80 (4.3 wt %)	17.5	−74.1	14.8	−72.0
100 (3.1 wt %)	2.5	–	−8.0	−81.3

References

1. Tanaka, G. Y.; May, C. A. Epoxy Resins Chemistry and Technology 1975; Vol. 1.
2. Lee, H.; Neville, K. Handbook of Epoxy Resins; The Epoxylite Corp.: South El Monte, CA, 1975; Chapters 1–4.
3. Sultan, J. N.; McGarry, F. J. Microstructure characteristics of toughened thermoset polymers, Cambridge, MIT, Research Report, 1996, 69.
4. Zhang, B-L.; Zhang, H. Q.; You, Y. C.; Du, Z. J.; Ding, P. Y.; Wang, T.; Huang, J. F. J Polym Sci 1998, 69, 339.

5. Ellis, R. L.; Lalande, F.; Jia, H. Y.; Rogers, C. A. J Reinforced Plast Compos 1998, 17, 147.
6. Oertel, C. Polyurethane Handbook; Hanser: Munich, 1985.
7. Iimura, K.; Koide, N.; Tanabe, H.; Takeda M. Makromol Chem 1981, 182, 2569.
8. Pohl, M. M.; Dany, R.; Mix, R.; Gahde J. Polymer 1996, 37, 2173.
9. Stenhouse, P. J.; Valles, E. M.; Kantor, S. W.; Macknight, W. J. Macromolecules 1989, 22, 1467.
10. Smyth, G.; Pollack, S. K.; Macknight, W. J.; Hsu, S. L. Liq Cryst 1990, 7, 839.
11. Khan, N.; Patel, V. L.; Bashir, Z.; Price, D. M. J Polym Sci Part B: Polym Phys 1995, 33, 1957.
12. Bashir, Z.; Khan, N. J Polym Sci Part B: Polym Phys 1996, 34, 2077.
13. Schartel, B.; Wendorff, J. H. Polym Eng Sci 1999, 39, 128.
14. Zhang, H.; Wang, B.; Li, H.; Jiang, Y.; Wang, J. Polym Int 2003, 52, 1493.
15. Hsieh, K. H.; Han, J. L. J Polym Sci Part B: Polym Phys 1990, 28, 623.
16. Hsieh, K. H.; Han, J. L. J Polym Sci Part B: Polym Phys 1990, 28, 783.
17. Tsou, L.; Sauer, J. A.; Hara, M. Polymer 2000, 41, 8103.
18. Tsou, L.; Sauer, J. A.; Hara, M. J Polym Sci Part B: Polym Phys 1999, 37, 2201.
19. Tsou, L.; Sauer, J. A.; Hara, M. J Polym Sci Part B: Polym Phys 2000, 38, 1377.
20. Cassidy, E. F.; Xiao, H. X.; Frisch, K. C.; Frisch, H. L. J Polym Sci: Polym Chem Ed 1984, 22, 1839.
21. Cassidy, E. F.; Xiao, H. X.; Frisch, K. C.; Frisch, H. L. J Polym Sci: Polym Chem Ed 1984, 22, 1851.
22. Cassidy, E. F.; Xiao, H. X.; Frisch, K. C.; Frisch, H. L. J Polym Sci: Polym Chem Ed 1984, 22, 2667.
23. Han, J. L.; Tseng, S. M.; Mai, J. H.; Hsieh, K. H. Die Angewandte Makromolekulare Chemie 1990, 184, 89.
24. Mahesh, K. P. O.; Alagar, M.; Kumar, S. A. Polym Adv Technol 2003, 14, 137.
25. Hsieh, K. H.; Han, J. L.; Yu, C. T.; Fu, S. C. Polymer 2001, 42, 2491.
26. Hepburn, C. Polyurethane Elastomers; Applied Science: London, 1982.
27. Han, J. L.; Tseng, S. M.; Mai, J. H.; Hsieh, K. H. Die Angewandte Makromolekulare Chemie 1990, 182, 193.